© 2014. Published by The Company of Biologists Ltd | Development (2014) 141, 909-917 doi:10.1242/dev.103093

RESEARCH ARTICLE

TGFβ regulates epithelial-mesenchymal interactions through WNT signaling activity to control muscle development in the soft palate

Jun-ichi Iwata[1,2], Akiko Suzuki[1], Toshiaki Yokota[1], Thach-Vu Ho[1], Richard Pelikan[1], Mark Urata[1,3], Pedro A. Sanchez-Lara[1,4,5] and Yang Chai[1,*]

ABSTRACT

Clefting of the soft palate occurs as a congenital defect in humans and adversely affects the physiological function of the palate. However, the molecular and cellular mechanism of clefting of the soft palate remains unclear because few animal models exhibit an isolated cleft in the soft palate. Using three-dimensional microCT images and histological reconstruction, we found that loss of TGFβ signaling in the palatal epithelium led to soft palate muscle defects in *Tgfbr2*$^{fl/fl}$*;K14-Cre* mice. Specifically, muscle mass was decreased in the soft palates of *Tgfbr2* mutant mice, following defects in cell proliferation and differentiation. Gene expression of Dickkopf (*Dkk1* and *Dkk4*), negative regulators of WNT–β-catenin signaling, is upregulated in the soft palate of *Tgfbr2*$^{fl/fl}$*;K14-Cre* mice, and WNT–β-catenin signaling is disrupted in the palatal mesenchyme. Importantly, blocking the function of DKK1 and DKK4 rescued the cell proliferation and differentiation defects in the soft palate of *Tgfbr2*$^{fl/fl}$*;K14-Cre* mice. Thus, our findings indicate that loss of TGFβ signaling in epithelial cells compromises activation of WNT signaling and proper muscle development in the soft palate through tissue-tissue interactions, resulting in a cleft soft palate. This information has important implications for prevention and non-surgical correction of cleft soft palate.

KEY WORDS: Cleft soft palate, TGFβ, Epithelial-mesenchymal interactions, Mouse

INTRODUCTION

The soft palate plays important roles in swallowing, speech, hearing, middle-ear ventilation and respiration (Back et al., 2004; Evans et al., 2010; Marsh, 1991). Despite the important physiological functions of the soft palate, we know very little about the mechanisms that regulate mammalian soft palate development (Bush and Jiang, 2012; Chai and Maxson, 2006). A failure of soft palate development results in a cleft soft palate and a risk of speech problems, middle ear disease and swallowing difficulties (Carvajal Monroy et al., 2012; Precious and Delaire, 1993).

The fleshy soft palate, which makes up approximately the posterior one-third of the secondary palate, is composed of muscles, whereas the anterior two-thirds consists of the bony hard palate (Hilliard et al., 2005; Iwata et al., 2011). Clinically, individuals with a cleft in the soft palate exhibit mis-orientation and delayed development of the soft palate muscles (Cohen et al., 1994). Even after surgical correction of the cleft soft palate and reconstruction of the muscle sling, there are often functional defects in the muscles (Flores et al., 2010; van der Sloot, 2003). Therefore, patients with a defect in the soft palate need long-term therapy and additional surgical corrections after the initial surgical repair for optimal function and normal speech development (Dworkin et al., 2004; Perry, 2011).

There are five muscles in the soft palate: the tensor veli palatini (TVP), the levator veli palatini (LVP), the palatoglossus, the palatopharyngeus and the musculus uvulae (Evans et al., 2010). Their formation, like that of limb and other craniofacial muscles, is controlled by regulatory processes distinct from those governing axial muscle formation (Grenier et al., 2009). The anatomical configuration of the soft palate muscles supports its unique physiological function. Surgical repair of cleft soft palate focuses on the LVP, which is the largest muscle in the soft palate and functions in its elevation (Evans et al., 2010). The LVP may become severely atrophic because of reduced function, and often is only half as thick in cleft soft palate patients as in healthy newborns. The other muscles in the soft palate have not been well studied.

Non-cell-autonomous activation of myogenesis in different regions of the embryo is controlled by a series of complex growth factor networks and niches that ultimately result in the expression of myogenic regulatory factors within nascent and differentiating myoblasts (Snider and Tapscott, 2003). Several epithelial-specific conditional knockout mice, such as *Shh*$^{c/n}$*;K14-Cre* and *Catnb*$^{fl/fl}$*;K14-Cre*, exhibit complete cleft palate and a cell proliferation defect in palatal mesenchymal cells, suggesting that oral epithelium-derived factors probably contribute to the cell fate determination of mesenchymal cells through tissue-tissue interactions during soft palate development (He et al., 2011; Lan and Jiang, 2009). In this study, we investigated how loss of transforming growth factor, beta receptor II (*Tgfbr2*) in the epithelium results in a cleft in the soft palate.

Transforming growth factor, beta (TGFβ; TGFβ1 – Mouse Genome Informatics) signaling plays a crucial role in craniofacial development. TGFβ transmits signals through TGFβ type I and type II receptors that phosphorylate SMAD2 and SMAD3, followed by the formation of transcriptional complexes with SMAD4 and translocation into the nucleus (Massagué and Chen, 2000). In addition, SMAD-independent pathways transduce TGFβ signals in some physiological and pathological conditions (Derynck and Zhang, 2003; Iwata et al., 2012; Xu et al., 2008). TGFβ ligands

[1]Center for Craniofacial Molecular Biology, Ostrow School of Dentistry, University of Southern California, Los Angeles, CA 90033, USA. [2]Center for Craniofacial Research, Department of Diagnostic and Biomedical Sciences, School of Dentistry, The University of Texas Health Science Center at Houston, TX 77054, USA. [3]Division of Plastic Surgery, Children's Hospital Los Angeles, Los Angeles, CA 90027, USA. [4]Department of Pediatrics, Keck School of Medicine, University of Southern California, Los Angeles, CA 90027, USA. [5]Division of Medical Genetics, Children's Hospital Los Angeles, Los Angeles, CA 90027, USA.

*Author for correspondence (ychai@usc.edu)

Received 26 August 2013; Accepted 4 December 2013

Development (2014) doi:10.1242/dev.103093

target a variety of genes in a developmental stage-dependent and cell-type-specific manner (Chai and Maxson, 2006; Iwata et al., 2011). Mice with loss of *Tgfbr2* in epithelial cells (*Tgfbr2*$^{fl/fl}$*;K14-Cre*) exhibit both submucous cleft palate and cleft soft palate. Our previous studies showed that TGFβ signaling regulates gene expression of *Irf6* and the fate of the medial edge epithelium (MEE) during palatal fusion in mice (Xu et al., 2006). Interestingly, overexpression of *Irf6* fails to rescue cleft soft palate in *Tgfbr2*$^{fl/fl}$*;K14-Cre* mice although it rescues submucous cleft palate and eliminates MEE persistence, suggesting that TGFβ may regulate the disappearance of the MEE through a different signaling network than the one it uses to control soft palate muscle development (Iwata et al., 2013a). However, it remains unknown how loss of TGFβ signaling in epithelial cells causes cleft soft palate and how mesoderm-derived muscle cells are affected.

In this study, we investigated the genetic basis of muscle formation and the cellular mechanism that controls muscle development in the soft palate during embryogenesis. We show that epithelial-specific loss of *Tgfbr2* results in cleft soft palate, compromised WNT signaling due to upregulated Dickkopf-related proteins 1 and 4 (DKK1 and DKK4), and muscle deformities in the soft palate of *Tgfbr2*$^{fl/fl}$*;K14-Cre* mice. Treatment with neutralizing antibodies for DKK1 and DKK4 rescued the mesenchymal cell proliferation and muscle development defects in an *ex vivo* organ culture system. Thus, our data indicate that impaired epithelial-mesenchymal communication contributes to the pathology of cleft soft palate.

RESULTS

Muscle deformation in the soft palate of *Tgfbr2*$^{fl/fl}$*;K14-Cre* mice

Loss of TGFβ signaling in the epithelium of *Tgfbr2*$^{fl/fl}$*;K14-Cre* mice resulted in cleft soft palate with a phenotype penetrance of 100% (Fig. 1A,B). We performed three-dimensional (3D) microCT imaging analysis to examine muscle formation in the soft palate and found that the TVP and LVP muscles were reduced in volume in newborn *Tgfbr2*$^{fl/fl}$*;K14-Cre* mice compared with wild-type littermate controls (Fig. 1C-J; supplementary material Fig. S1). In addition, we generated 3D histological images of the soft palate of *Tgfbr2*$^{fl/fl}$*;K14-Cre* and wild-type control mice (Fig. 1K-P). The TVP and LVP muscles in *Tgfbr2*$^{fl/fl}$*;K14-Cre* mice were smaller than those in wild-type controls. We concluded from these results that the development of the TVP and LVP are compromised in newborn *Tgfbr2*$^{fl/fl}$*;K14-Cre* mice as the result of loss of TGFβ signaling in the palatal epithelium.

Next, we investigated the time course of muscle development in the soft palate from embryonic day (E)14.5 to E18.5 (Fig. 2A-H). Although we first detected myofibers in the soft palate of both *Tgfbr2*$^{fl/fl}$*;K14-Cre* and wild-type control mice at E15.5, the total volume of the muscle in the soft palate was reduced in *Tgfbr2*$^{fl/fl}$*;K14-Cre* mice compared with wild-type control mice. At E15.5 and later embryonic stages, *Tgfbr2*$^{fl/fl}$*;K14-Cre* mice exhibited a cleft in the soft palate, consistent with the reduction of muscle volume in the soft palate (Fig. 2I-R; supplementary material Fig.

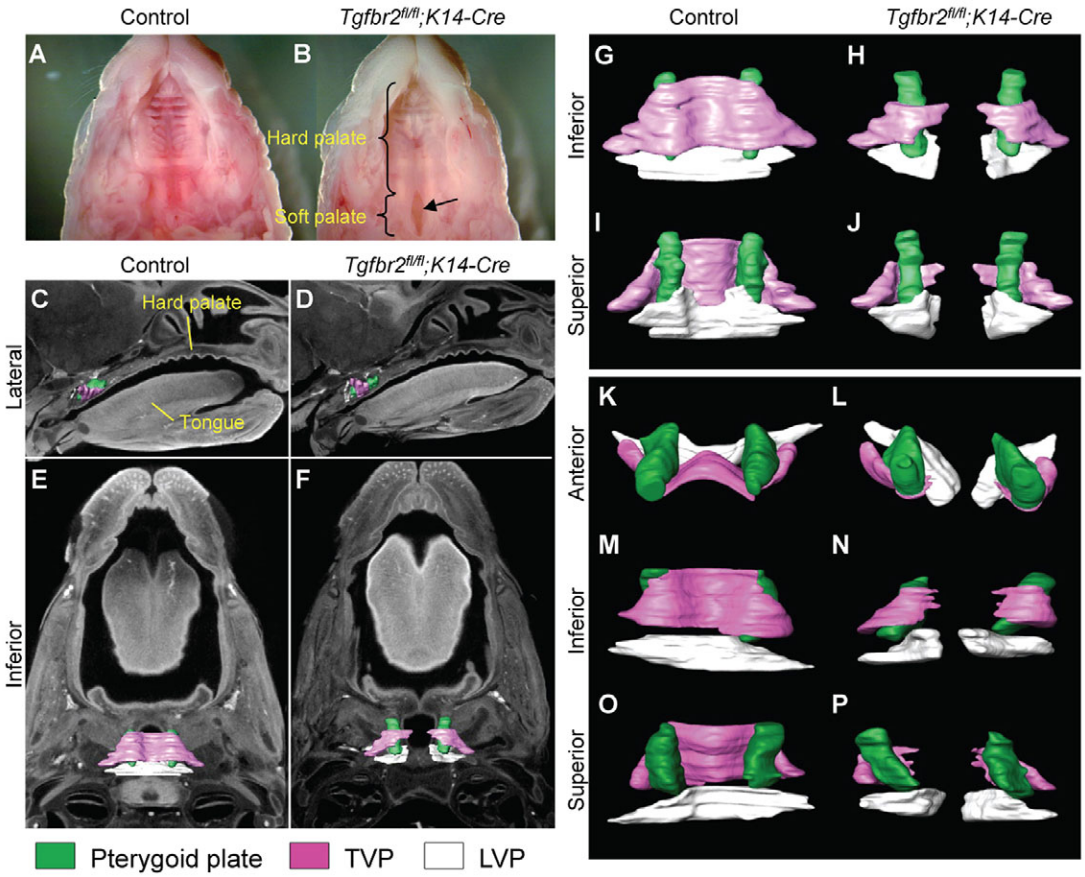

Fig. 1. Epithelial-specific loss of *Tgfbr2* in mice results in muscle mass reduction and cleft soft palate. (A,B) Macroscopic appearance of palates of newborn *Tgfbr2*$^{fl/fl}$ control and *Tgfbr2*$^{fl/fl}$*;K14-Cre* mice. Arrow indicates cleft soft palate. (C-J) 3D reconstruction of palates from microCT images of E18.5 *Tgfbr2*$^{fl/fl}$ control (C,E,G,I) and *Tgfbr2*$^{fl/fl}$*;K14-Cre* mice (D,F,H,J). Pterygoid plate (green); TVP (tensor veli palatini, pink); LVP (levator veli palatini, white). (K-P) 3D reconstruction of palates from histological sections of E18.5 *Tgfbr2*$^{fl/fl}$ control (K,M,O) and *Tgfbr2*$^{fl/fl}$*;K14-Cre* mice (L,N,P). Pterygoid plate (green); TVP (pink); LVP (white).

Development (2014) doi:10.1242/dev.103093

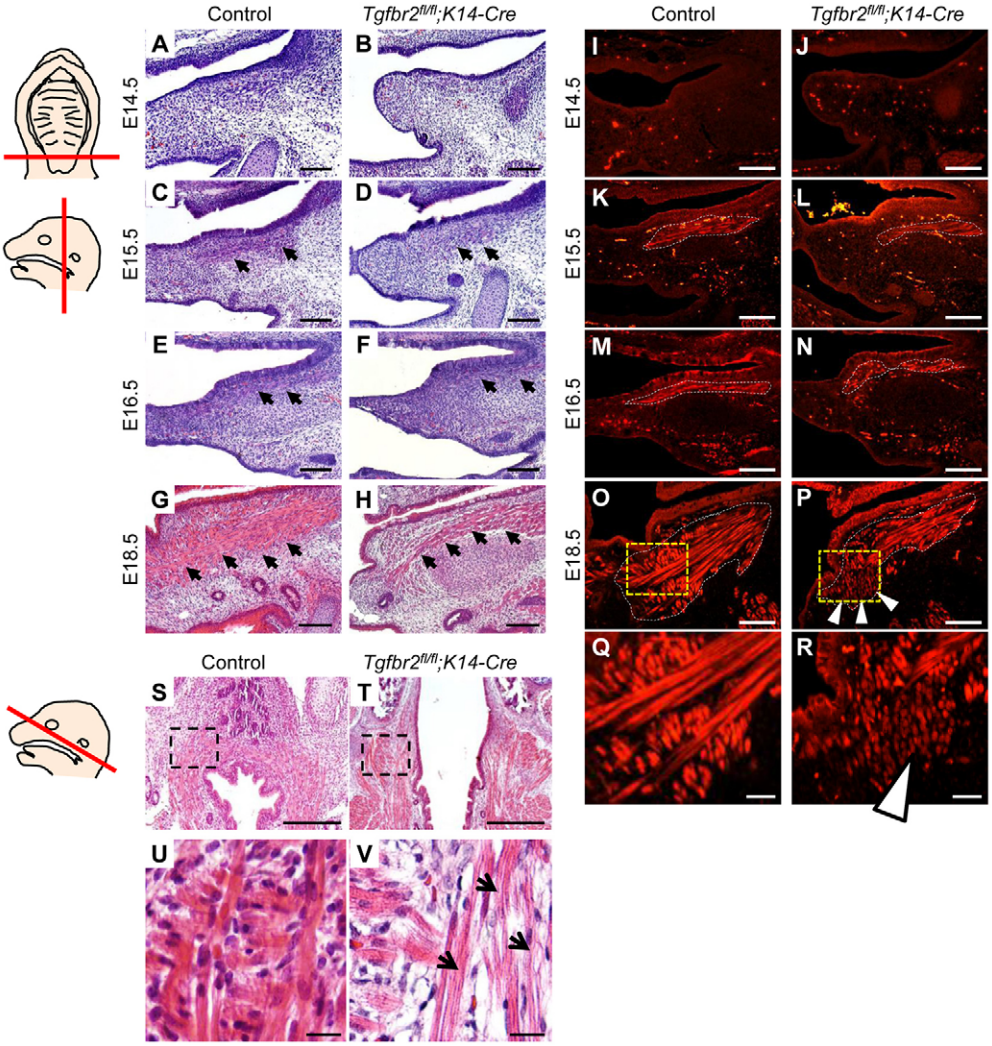

Fig. 2. Reduction of muscle mass in *Tgfbr2$^{fl/fl}$;K14-Cre* mice. (A-H) H&E staining of *Tgfbr2$^{fl/fl}$* control (A,C,E,G) and *Tgfbr2$^{fl/fl}$;K14-Cre* (B,D,F,H) mice at the indicated developmental stages. Red lines on the schematic drawings on the left show the position of the sections. Arrows indicate the LVP. Scale bars: 100 μm. (I-R) Immunohistochemical staining of myosin heavy chain (MyHC) in the soft palate of *Tgfbr2$^{fl/fl}$* control (I,K,M,O,Q) and *Tgfbr2$^{fl/fl}$;K14-Cre* (J,L,N,P,R) mice at the indicated developmental stages. Dotted lines indicate outline of the LVP. Arrowheads indicate altered orientation of muscle fibers. Boxed areas in O and P are enlarged in Q and R, respectively. Scale bars: 100 μm (I-P); 25 μm (Q,R). (S-V) H&E staining of E18.5 *Tgfbr2$^{fl/fl}$* control (S,U) and *Tgfbr2$^{fl/fl}$;K14-Cre* (T,V) mice. Boxed areas in S and T are enlarged in U and V, respectively. Red line on the schematic on the left indicates the position of the sections. Arrows indicate muscle atrophy. Scale bars: 100 μm (S,T); 10 μm (U,V).

S2). In addition, the muscle fibers were aligned in the anterior-posterior direction in the soft palate of *Tgfbr2$^{fl/fl}$;K14-Cre* mice, in contrast to the lateral-medial alignment in controls. Moreover, the muscles in *Tgfbr2$^{fl/fl}$;K14-Cre* mice were attached to the posterior border of the hard palate, similar to human patients with a cleft in the soft palate. We also found that muscle fibers in *Tgfbr2$^{fl/fl}$;K14-Cre* mice were thinner than in control mice, suggesting that *Tgfbr2$^{fl/fl}$;K14-Cre* mice may have a defect in the maturation of myotubes into myofibers (Fig. 2S-V). Collectively, these findings indicate that *Tgfbr2$^{fl/fl}$;K14-Cre* mice can serve as an excellent model to investigate the mechanism that regulates soft palate development and associated malformations.

To analyze the mechanism that causes cleft soft palate in *Tgfbr2$^{fl/fl}$;K14-Cre* mice, we investigated cell proliferation and apoptosis activities. We found that cell proliferation was reduced in *Tgfbr2$^{fl/fl}$;K14-Cre* mice at E14.5 and E15.5 (Fig. 3) but apoptosis was unaffected (supplementary material Fig. S3). Next, we investigated whether muscle differentiation and maturation were altered in the soft palate of *Tgfbr2$^{fl/fl}$;K14-Cre* mice. We found that myofibers were thin and disorganized, appearing wavy and lacking striation (Fig. 4A,B). The diameter of myofibers was decreased in *Tgfbr2$^{fl/fl}$;K14-Cre* mice (Fig. 4C). In addition, the percentage of centrally placed nuclei in myofibers was significantly increased ($P<0.05$) in *Tgfbr2$^{fl/fl}$;K14-Cre* mice compared with wild-type control mice (Fig. 4D-H). Taken together, our data indicate that failure of muscle cell proliferation and differentiation probably leads to muscle defects and cleft soft palate in *Tgfbr2$^{fl/fl}$;K14-Cre* mice.

Molecular mechanisms of cleft soft palate formation in *Tgfbr2$^{fl/fl}$;K14-Cre* mice

To explore the molecular mechanism of cleft soft palate formation in *Tgfbr2$^{fl/fl}$;K14-Cre* mice, we performed global gene expression analysis using soft palate tissue from *Tgfbr2$^{fl/fl}$;K14-Cre* and wild-type control mice at E15.5 (n=6 per genotype) and examined the downstream consequences of dysfunctional TGFβ signaling in epithelial cells. In this comparison, we uncovered 291 probe sets representing transcripts that were differentially expressed [≥1.5-fold, <5% false discovery rate (FDR)], 148 of them more abundant in *Tgfbr2$^{fl/fl}$;K14-Cre* mice (supplementary material Table S1) and 143 more abundant in wild-type control mice (supplementary material Table S2; see http://face.usc.edu//category/microarrays/). The genes identified were consistent with muscle defects, with significant reductions in the levels of transcripts related to the control of muscle movement, such as motoneurons, muscular metabolism and channel molecules for ion exchange (supplementary material Table S2). In order to examine how epithelial-specific deletion of *Tgfbr2* results in defects in muscle formation, we focused on the expression of genes related to growth differentiation factors as candidates for regulating tissue-tissue interactions. We found that transcript levels of *Dkk1* and *Dkk4*, which are negative regulators of WNT–β-catenin signaling,

Development (2014) doi:10.1242/dev.103093

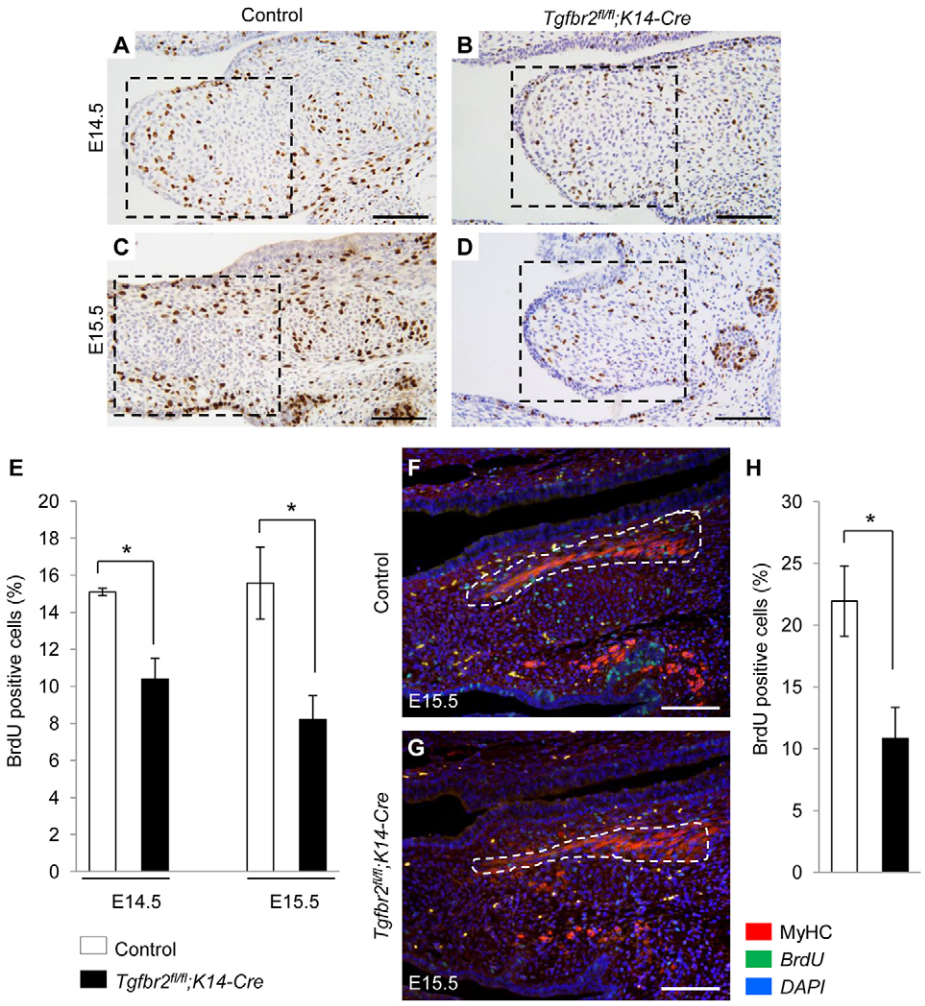

Fig. 3. Cell proliferation defect in the soft palate of *Tgfbr2$^{fl/fl}$;K14-Cre* mice. (A-D) BrdU staining (brown) of *Tgfbr2$^{fl/fl}$* control (A,C) and *Tgfbr2$^{fl/fl}$;K14-Cre* (B,D) mice at E14.5 and E15.5. Scale bars: 100 µm. (E) Quantification of the number of BrdU-labeled nuclei in the palates of *Tgfbr2$^{fl/fl}$* control (white bars) and *Tgfbr2$^{fl/fl}$;K14-Cre* (black bars) mice at E14.5 and E15.5. Three samples per genotype were analyzed. **P*<0.05; *n*=3. (F-H) Immunofluorescence images of BrdU (green) and MyHC (red) staining in the LVP of *Tgfbr2$^{fl/fl}$* control (F) and *Tgfbr2$^{fl/fl}$;K14-Cre* (G) mice at E15.5. Nuclei were counterstained with DAPI (blue). The number of BrdU-labeled nuclei is quantified in H. Three samples per genotype were analyzed. **P*<0.05. Dotted lines indicate outline of the LVP. Scale bars: 100 µm.

were significantly increased (*Dkk1*: 2.4-fold change, FDR=0.0448; *Dkk4*: 5.6-fold change, FDR=0.0103) in the soft palate of *Tgfbr2$^{fl/fl}$;K14-Cre* mice (supplementary material Table S1). We confirmed the increased gene expression levels of *Dkk1* and *Dkk4* in E15.5 *Tgfbr2$^{fl/fl}$;K14-Cre* mice by quantitative RT-PCR analysis (Fig. 5A). In order to investigate gene expression patterns of *Dkk1* and *Dkk4*, we performed whole-mount *in situ* hybridization for *Dkk1* and *Dkk4*. We detected ectopic expression in the posterior palate of E14.0 *Tgfbr2$^{fl/fl}$;K14-Cre* mice (Fig. 5B-E). We also performed section *in situ* hybridization of *Dkk1* and *Dkk4* in E15.5 *Tgfbr2$^{fl/fl}$;K14-Cre* and wild-type control mice (Fig. 5F-I). *Dkk1* and *Dkk4* gene expression was restricted to the epithelial layers and was not detectable in the palatal mesenchyme of *Tgfbr2$^{fl/fl}$;K14-Cre* mice. Next, we performed immunohistological analysis for DKK1 (Fig. 5J-Q), and found that DKK1 expression was increased in the mesenchyme of *Tgfbr2$^{fl/fl}$;K14-Cre* mice compared with wild-type control mice. DKK1 expression was detectable in the MEE in both wild-type control and *Tgfbr2$^{fl/fl}$;K14-Cre* mice at E14.5. At E15.5, the MEE started to dissociate and DKK1 expression decreased in wild-type control mice. By contrast, DKK1 expression persisted in *Tgfbr2* mutant MEE cells, and its expression was increased in the palatal mesenchyme (Fig. 5J-Q). To confirm the diffusion of DKK1 protein to the mesenchyme, we isolated palatal mesenchyme from the soft palate of E15.5 control and *Tgfbr2$^{fl/fl}$;K14-Cre* mice and performed immunoblotting analysis for DKK1 (Fig. 5R). We found that DKK1 protein was undetectable in the palatal mesenchyme from wild-type control mice. By contrast, we detected DKK1 expression in the palatal mesenchyme of *Tgfbr2$^{fl/fl}$;K14-Cre* mice. Next, to investigate whether overexpression of DKK1 affected WNT activity in *Tgfbr2$^{fl/fl}$;K14-Cre* mice, we performed immunoblotting analysis using samples from the entire E15.5 soft palate (Fig. 6A,B). In *Tgfbr2$^{fl/fl}$;K14-Cre* mice, DKK1 expression level was significantly upregulated. Moreover, we detected a decrease in the expression of the active form of β-catenin (ABC) and an increase in phosphorylated β-catenin in *Tgfbr2$^{fl/fl}$;K14-Cre* mice compared with wild-type control mice. Taken together, our data indicate that upregulated DKK1 in the palatal epithelium resulted in compromised WNT activity in the palatal mesenchyme during soft palate development.

Rescue of muscle cell proliferation and differentiation in *Tgfbr2$^{fl/fl}$;K14-Cre* soft palate

We hypothesized that inhibition of WNT signaling activity might cause defects in cell proliferation and differentiation of muscle cells, because previous studies have shown that WNT signaling is important in muscle development (Snider and Tapscot, 2003). To test this hypothesis, we cultured C2C12 cells, a mouse myoblast cell line, in proliferation or differentiation medium with or without an inhibitor for canonical WNT–β-catenin signaling (endo-IWR1). We found that endo-IWR1 suppressed cell proliferation activity in C2C12 cells (Fig. 7A). Similarly, endo-IWR1 inhibited cell proliferation activity in primary cranial neural crest (CNC)-derived MEPM cells from wild-type mice (Fig. 7B). Next, in order to test

Development (2014) doi:10.1242/dev.103093

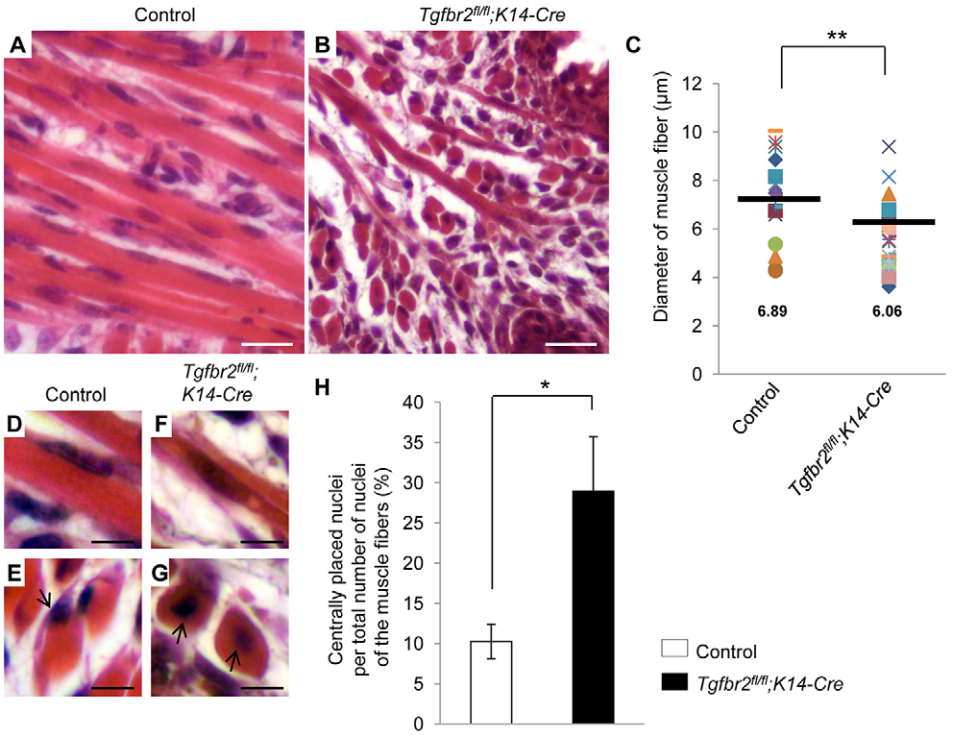

Fig. 4. Altered differentiation of myogenic cells in *Tgfbr2$^{fl/fl}$;K14-Cre* mice. (A,B) H&E staining of LVP from E18.5 *Tgfbr2$^{fl/fl}$* control (A) and *Tgfbr2$^{fl/fl}$;K14-Cre* (B) mice. Scale bars: 20 μm. (C) Quantification of the diameter of muscle fibers in the palates of E18.5 control and *Tgfbr2$^{fl/fl}$;K14-Cre* mice. Horizontal bars indicate the mean (stated below). ***P*<0.01; *n*=6. (D-G) Representative high magnification images of centrally placed nuclei in the longitudinal (D,F) or coronal (E,G) directions in A and B. Arrows indicate nuclei. Scale bars: 10 μm. (H) Quantification of the number of centrally placed nuclei out of the total number of nuclei in the muscle fibers of E18.5 control (white bar) and *Tgfbr2$^{fl/fl}$;K14-Cre* (black bar) palates. Three samples per genotype were analyzed. **P*<0.05.

whether WNT–β-catenin signaling is crucial for muscle differentiation, we cultured C2C12 cells in differentiation medium for 0, 3 or 5 days. We found that endo-IWR1 inhibited muscle differentiation in C2C12 cells (Fig. 7C-H). Moreover, we cultured wild-type palatal explants with endo-IWR1 for 1 or 3 days (Fig. 8A-J). Strikingly, wild-type palates treated with endo-IWR1 in an *ex vivo* organ culture system (Fig. 8B,E,H) mimicked the cell proliferation and differentiation defects in *Tgfbr2$^{fl/fl}$;K14-Cre* palates (Fig. 8C,F,I), whereas these activities were not affected after treatment with vehicle (Fig. 8A,D,G). Thus, our data indicate that WNT signaling is crucial for soft palate muscle development.

We hypothesized that reduction of DKK1 and DKK4 would rescue the defective cell proliferation and muscle differentiation activities in *Tgfbr2$^{fl/fl}$;K14-Cre* mice. To test this hypothesis, we treated palatal explants from *Tgfbr2$^{fl/fl}$;K14-Cre* mice with neutralizing antibodies (NAb) for DKK1 and DKK4 (Fig. 9A-J). We found that treatment with NAb for DKK1 and DKK4 could rescue the cell proliferation defect in the mesenchyme of *Tgfbr2$^{fl/fl}$;K14-Cre* palates (Fig. 9A-C,J). Similarly, treatment with NAb for DKK1 and DKK4 could rescue both muscle cell proliferation and differentiation defects in *Tgfbr2$^{fl/fl}$;K14-Cre* palates in an *ex vivo* organ culture system (Fig. 9D-J). Collectively, our findings indicate that inhibition of WNT signaling through elevated DKK1 and DKK4 expression is responsible for the failure of soft palate development and the muscle defects in *Tgfbr2$^{fl/fl}$;K14-Cre* mice (Fig. 9K).

DISCUSSION

Our mouse model for cleft soft palate, *Tgfbr2$^{fl/fl}$;K14-Cre*, suggests that specific regulators, such as growth factors, from epithelial cells may control the fate and orientation of muscle cells during palatogenesis. Importantly, this mutant mouse model mimics the phenotype of human individuals with cleft soft palate. Using the mouse model, we explored how loss of TGFβ signaling in epithelial cells results in a failure of muscle development and found that TGFβ-controlled WNT–β-catenin signaling activity is crucial for muscle formation. Previous studies indicated that DKK1 and DKK4 can inhibit WNT–β-catenin signaling (Kawano and Kypta, 2003; Nie et al., 2005; Semënov et al., 2001). *Dkk1* knockout mice exhibit severe craniofacial deformities and embryonic lethality before palatal development (Mukhopadhyay et al., 2001). Mice lacking β-catenin in CNC-derived cells (*Catnb$^{fl/fl}$;Wnt1-Cre*) exhibit severe craniofacial deformities (Brault et al., 2001), and *Wnt9b* knockout mice exhibit cleft palate (Jin et al., 2012). Thus, WNT signaling is involved in craniofacial development. Loss of WNT–β-catenin signaling results in downregulation of TGFβ, whereas expression of stabilized β-catenin in the palatal epithelium causes ectopic *Tgfb3* expression and fusion of the palatal shelf and mandible (He et al., 2011). Our study clearly shows that TGFβ signaling also affects WNT signaling activity through DKK1 and DKK4. This feedback between TGFβ and WNT signaling may be crucial for maintaining normal growth factor signaling during craniofacial development.

Tgfbr2$^{fl/fl}$;K14-Cre mice exhibit both persistence of the MEE in the hard palate (submucous cleft palate) and a cleft in the soft palate (cleft soft palate). Our previous studies showed that TGFβ signaling regulates *Irf6* gene expression and the fate of the MEE, and overexpression of *Irf6* rescues MEE disappearance although it fails to rescue the cleft in the soft palate in *Tgfbr2$^{fl/fl}$;K14-Cre* mice, indicating that the molecular mechanism of soft palate development is different from that of MEE fate determination (supplementary material Fig. S4) (Iwata et al., 2013a; Xu et al., 2006). *Irf6* is only expressed in palatal epithelial cells (Iwata et al., 2013a; Thomason et al., 2010). Hence, TGFβ regulated IRF6 signaling must only control the fate of MEE cells, and other TGFβ downstream targets must control other aspects of palate development. This reasoning is supported by our finding that *Dkk1* and *Dkk4* expression is specifically upregulated in the posterior palate of *Tgfbr2$^{fl/fl}$;K14-Cre* mice, resulting in compromised WNT–β-catenin signaling activity in the mesenchyme and soft palate muscle defects. These results suggest that TGFβ signaling plays a crucial role in regulating tissue-tissue interactions during palatogenesis. In order to investigate this further,

Development (2014) doi:10.1242/dev.103093

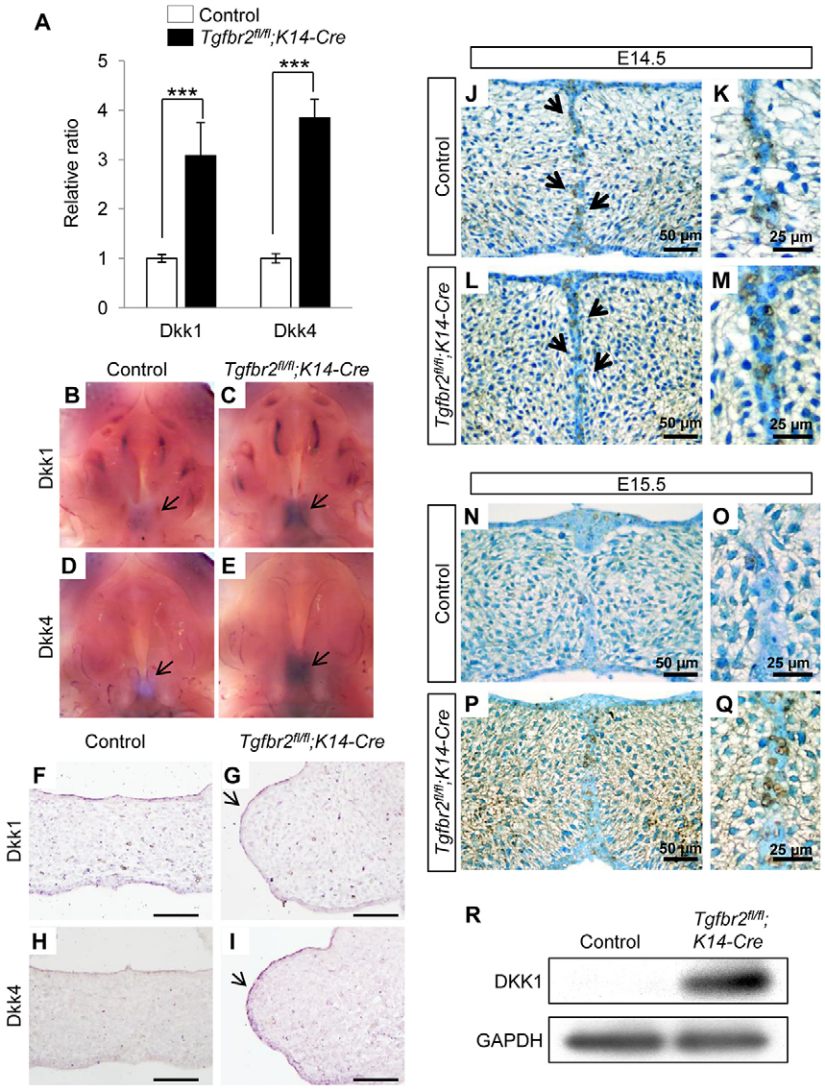

Fig. 5. Identification of molecules altered in the soft palate of *Tgfbr2*$^{fl/fl}$*;K14-Cre* mice. (A) Quantitative RT-PCR analyses of the *Dkk1* and *Dkk4* genes in the soft palates of E15.5 *Tgfbr2*$^{fl/fl}$ control (white bars) and *Tgfbr2*$^{fl/fl}$*;K14-Cre* (black bars) mice. Three samples were analyzed for each experiment. ***P<0.001. (B-E) Whole-mount *in situ* hybridization for *Dkk1* (B,C) and *Dkk4* (D,E) in E14.0 *Tgfbr2*$^{fl/fl}$ control (B,D) and *Tgfbr2*$^{fl/fl}$*;K14-Cre* (C,E) palates. Arrows indicate positive signals (purple). (F-I) Section *in situ* hybridization for *Dkk1* (F,G) and *Dkk4* (H,I) in E15.5 *Tgfbr2*$^{fl/fl}$ control (F,H) and *Tgfbr2*$^{fl/fl}$*;K14-Cre* (G,I) mice. Arrows indicate positive signals (purple). Scale bars: 100 μm. (J-Q) Immunohistochemical analysis for DKK1 in *Tgfbr2*$^{fl/fl}$ control (J,K,N,O) and *Tgfbr2*$^{fl/fl}$*;K14-Cre* (L,M,P,Q) palates at E14.5 (J-M) and E15.5 (N-Q). Arrows indicate positive signals (brown). High magnification images from J,L,N,P are shown in K,M,O,Q, respectively. Scale bars: 50 μm in J,L,N,P; 25 μm in K,M,O,Q. (R) Immunoblotting analysis of DKK1 in palatal mesenchyme of E15.5 *Tgfbr2*$^{fl/fl}$ (control) and *Tgfbr2*$^{fl/fl}$*;K14-Cre* soft palate. GAPDH was used as a loading control.

we compared gene expression profiles of the anterior and posterior palate in E15.5 wild-type mice and found that a total of 887 transcripts were differentially expressed in the soft palate. We focused on the TGFβ signaling pathway and found that TGFβ signaling mediators were differentially expressed (supplementary material Fig. S5), suggesting that TGFβ signaling is differently regulated in the anterior versus posterior palate during palate formation. This putative asymmetry is supported by our previous finding that haploinsufficiency of *Tgfbr1/Alk5* in *Tgfbr2*$^{fl/fl}$*;Wnt1-Cre* mice failed to rescue soft palate development, whereas it rescued clefting of the hard palate (Iwata et al., 2012) (our unpublished data). Our previous studies indicate that SMAD and p38 mitogen-activated protein kinase (MAPK) are functionally redundant in regulating the fate of the MEE cells (Xu et al., 2006; Iwata et al., 2013a). Therefore, gene expression of *Dkk1* and *Dkk4* may be regulated by both canonical and non-canonical TGFβ signaling. We analyzed the promoter sequences of *Dkk1* and *Dkk4* and found that the promoter regions of both genes contain SMAD-binding sites and p38 MAPK response elements (data not shown). Taken together, our findings suggest that gene expression of *Dkk1* and *Dkk4* may be regulated by TGFβ signaling in a tissue- and region-specific manner.

In addition to epithelial signals, the defects in the muscle fibers in the soft palate could also be the result of improper signaling from the cranial neural crest (CNC)-derived palatal mesenchyme. In the

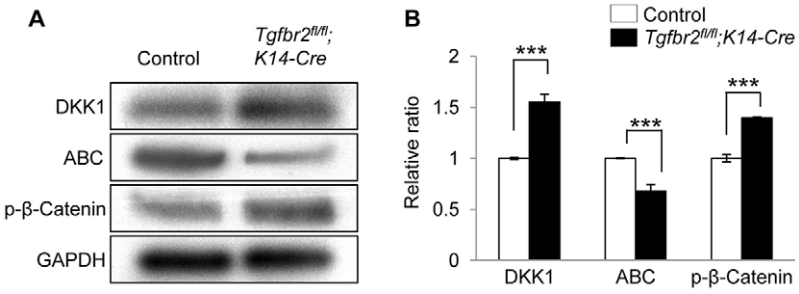

Fig. 6. Compromised WNT–β-catenin signaling activity in the soft palate of *Tgfbr2*$^{fl/fl}$*;K14-Cre* mice. (A,B) Immunoblotting analysis of DKK1, active form of β-catenin (ABC), and phosphorylated β-catenin (p-β-Catenin) in the entire soft palate of E15.5 *Tgfbr2*$^{fl/fl}$ (control) and *Tgfbr2*$^{fl/fl}$*;K14-Cre* mice. GAPDH was used as a loading control. Bar graph (B) shows the ratio of DKK1, ABC and p-β-catenin per GAPDH following quantitative densitometry analyses of immunoblots. White bars, *Tgfbr2*$^{fl/fl}$ control; black bars, *Tgfbr2*$^{fl/fl}$*;K14-Cre*. Three samples per genotype were analyzed. ***P<0.001.

Development (2014) doi:10.1242/dev.103093

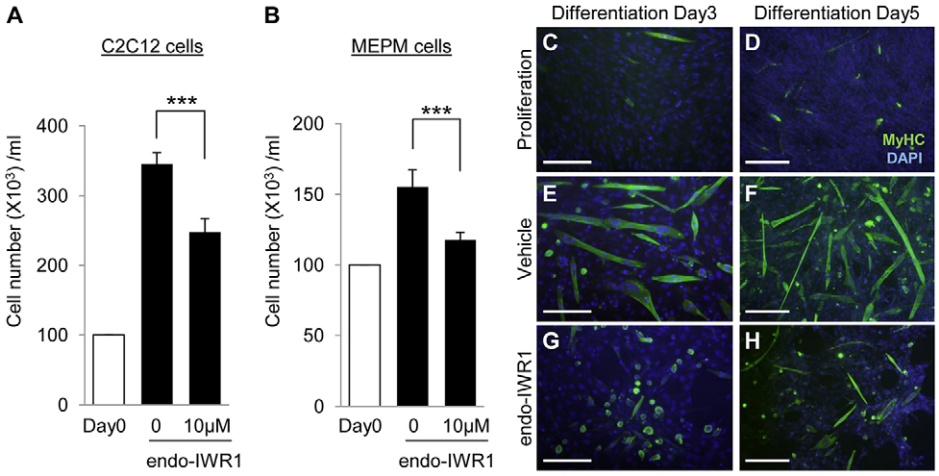

Fig. 7. Inhibition of WNT-signaling-compromised cell proliferation and differentiation activities. (A,B) Cell proliferation assays of C2C12 (A) and MEPM (B) cells after treatment with endo-IWR1 at 0 or 10 μM for 24 hours. ***P<0.001; n=6. (C-H) MyHC staining (green) with DAPI (blue) after treatment with vehicle or endo-IWR1 for the indicated number of days. Scale bars: 100 μm (C,E,G); 200 μm (D,F,H).

craniofacial region, CNC-derived cells give rise to tendons and connective tissues in the skeletal muscles, whereas these tissues are derived from the lateral mesoderm in the rest of body. CNC-specific *Tgfbr2* mutant (*Tgfbr2$^{fl/fl}$;Wnt1-Cre*) mice exhibit muscle abnormalities in the tongue (Iwata et al., 2013b) and soft palate (supplementary material Fig. S6), following defects in cell proliferation and maturation or organization. Moreover, in our microarray analyses of palates from E14.5 *Tgfbr2$^{fl/fl}$;Wnt1-Cre* mice (Iwata et al., 2012), we found that expression of genes in the WNT signaling pathway, including *Dkk2* and *Limd1*, was altered (supplementary material Figs S6, S7). Taken together, our results suggest an important positive role for CNC cells in craniofacial muscle development.

We found that elevated WNT inhibitors DKK1 and DKK4 diminished WNT–β-catenin signaling in the soft palate and adversely affected the proliferation and differentiation of myoblasts as well as the maturation of myotubes into myofibers in the palatal mesenchyme. These findings have important implications for clinical studies that aim to identify patients with cleft soft palate and families with a high risk of cleft soft palate. Moreover, this study lays the groundwork for efforts to reorient soft palate muscles and to accelerate muscle regeneration in patients with cleft soft palate. Our study of soft palate development could also be useful for understanding tissue-tissue interaction mechanisms in regulating skeletal muscle development and regeneration.

MATERIALS AND METHODS

Animals

To generate *Tgfbr2$^{fl/fl}$;K14-Cre* mice, we mated *Tgfbr2$^{fl/+}$;K14-Cre* with *Tgfbr2$^{fl/fl}$* mice. To generate *Tgfbr2$^{fl/fl}$;K14-Cre;Irf6^{Tg}* mice, we mated *Tgfbr2$^{fl/+}$;K14-Cre;Irf6^{Tg}* with *Tgfbr2$^{fl/fl}$* mice. To generate *Tgfbr2$^{fl/fl}$;Wnt1-Cre* mice, we mated T*gfbr2$^{fl/+}$;Wnt1-Cre* with *Tgfbr2$^{fl/fl}$* mice. Genotyping was performed using PCR primers as described previously (Iwata et al., 2012; Iwata et al., 2013a; Xu et al., 2006).

MicroCT analysis

MicroCT analysis was performed using a SCANCO μCT50 device at the University of Southern California Molecular Imaging Center. The microCT images were acquired with the X-ray source at 70 kVp and 114 μA. The data were collected at a resolution of 10 μm. The three-dimensional (3D) reconstruction was done with AVIZO 7.1 software (Visualization Sciences Group).

Microarray analysis

Total RNA samples (1 μg per sample) were isolated from E15.5 soft palate of control and *Tgfbr2$^{fl/fl}$;K14-Cre* mice, and converted into biotin-labeled cRNA using the GeneChip IVT Labeling Kit with Biotin-ddUTP and standard protocols recommended by Affymetrix (Santa Clara, CA, USA). Fragmented cDNA was applied to GeneChip Mouse Genome 430 2.0 Arrays (Affymetrix) containing probe sets designed to detect over 39,000 transcripts. Microarrays were hybridized, processed and scanned as previously described (Karaman et al., 2003), using the manufacturer's recommended conditions. WebArray software was used to generate scaled $\log_2$-transformed gene expression values using the RMA algorithm (Wang et al., 2009; Xia et al., 2005). Probes sets showing ≥1.5-fold differential expression with a <5% false discovery rate (FDR) were identified through liner models for microarray data (LIMMA)-based liner model statistical analysis (Smyth, 2004) and FDR calculations made using the spacings LOESS histogram (SPLOSH) method (Pounds and Cheng, 2004). All scaled gene expression scores and .cel files are available at the National Center for Biotechnology Information (NCBI) Gene Expression Omnibus (GEO) repository under the series accession number GSE46211.

Histological examination

Hematoxylin and Eosin (H&E), BrdU and immunohistochemical staining were performed as described previously (Iwata et al., 2010; Iwata et al., 2012; Iwata et al., 2013a). Antibodies used for immunohistochemistry were mouse monoclonal antibody against myosin heavy chain (MyHC; Sigma-Aldrich) and DKK1 (Santa Cruz Biotechnology). Fluorescence images were obtained using a fluorescence microscope (Model IX71, Olympus).

Quantitative RT-PCR

Total RNA was isolated from mouse soft palate dissected at E15.5 using QIAshredder and RNeasy Micro extraction kits (Qiagen), as described previously (Iwata et al., 2010). The following PCR primers were used: *Dkk1*, 5′-GAGGGGAAATTGAGGAAAGC-3′ and 5′-GGTGCACACCTG-ACCTTCTT-3′; *Dkk4*, 5′-TAGAGTTCGCAGGAGGTGTC-3′ and 5′-TGAGGTCTGTTTTCCTCTGC-3′; *Dkk2*, 5′-ACCCTTGCAGCAGTGA-TAAG-3′ and 5′-TGGCTTTGGAAGAGTAGGTG-3′; *Limd1*, 5′-CGGA-CTACTTCGGTTCCTGT-3′ and 5′-TTACAGATGACGCAGCGGAA-3′; and *Gapdh*, 5′-AACTTTGGCATTGTGGAAGG-3′ and 5′-ACACATTG-GGGGTAGGAACA-3′. A two-tailed Student's t-test was applied for statistical analysis of quantitative PCR data. A P-value ≤0.05 was considered statistically significant. For all graphs, data are means ± standard deviation (s.d.).

Immunoblotting analysis

Immunoblotting was performed as described previously (Iwata et al., 2012; Iwata et al., 2013b). Antibodies used for immunoblotting were as follows: mouse monoclonal antibodies against DKK1 (Santa Cruz Biotechnology), active form of β-catenin (ABC) and GAPDH (Millipore), and rabbit polyclonal antibody against phosphorylated β-catenin (Cell Signaling Technology).

Development (2014) doi:10.1242/dev.103093

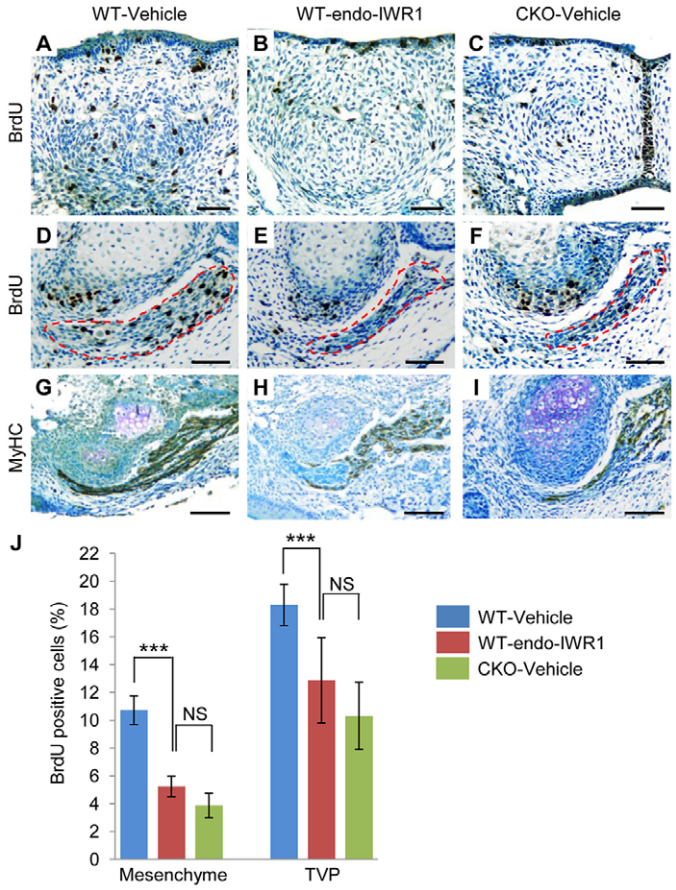

Fig. 8. Inhibition of WNT signaling causes cell proliferation and muscle differentiation defects in palatal explants. (A-C) BrdU staining after treatment with vehicle or endo-IWR1 for 1 day in palatal explants from wild-type mice (A,B) or treatment with vehicle in *Tgfbr2*$^{fl/fl}$*;K14-Cre* mice (C). Scale bars: 50 µm. (D-I) BrdU (D-F) and MyHC staining (G-I) after treatment with vehicle (D,G) or endo-IWR1 (E,H) for 3 days in palatal explants from wild-type mice (D,E,G,H) or treatment with vehicle in palatal explants from *Tgfbr2*$^{fl/fl}$*;K14-Cre* mice (F,I). Dotted lines indicate the outline of the TVP. Scale bars: 50 µm. (J) Quantification of the number of BrdU-labeled nuclei after treatment with vehicle (blue bars) or endo-IWR1 (red bars) in the mesenchyme or the TVP of wild-type palatal explants and treatment with vehicle in palatal explants from *Tgfbr2*$^{fl/fl}$*;K14-Cre* mice (green bars). Six samples per group were analyzed. ***P<0.001; NS, not significant.

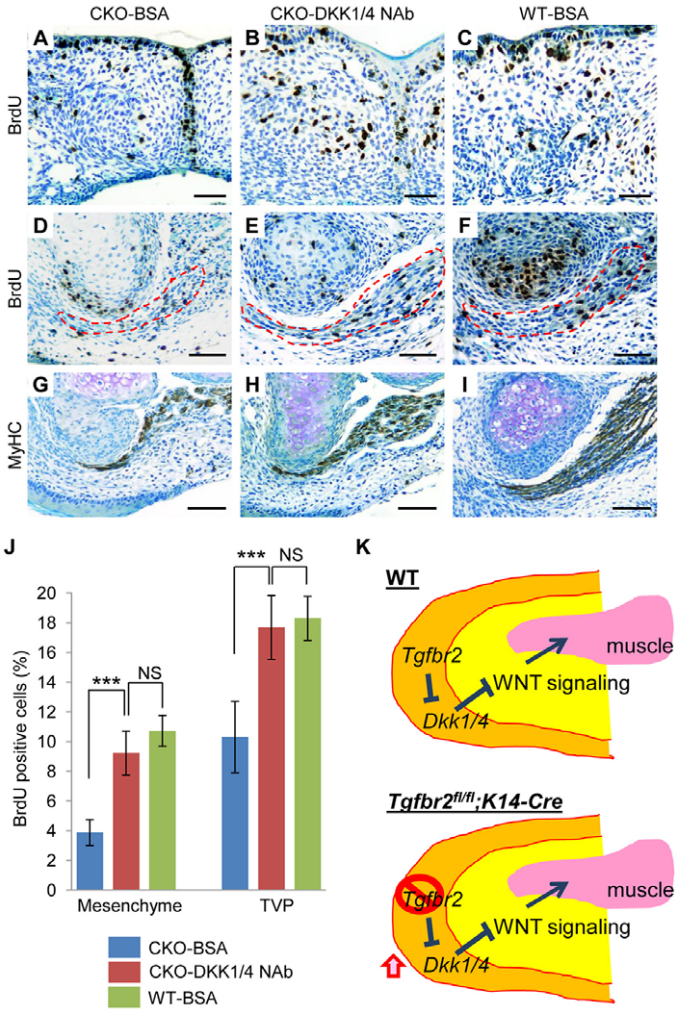

Fig. 9. Restored cell proliferation and muscle differentiation activities in the soft palate of *Tgfbr2*$^{fl/fl}$*;K14-Cre* mice. (A-C) BrdU staining after treatment with BSA (A) or neutralizing antibody (NAb) for DKK1 and DKK4 (B) for 1 day in *Tgfbr2*$^{fl/fl}$*;K14-Cre* soft palate explants and with BSA in *Tgfbr2*$^{fl/fl}$ control soft palate explants (C). Scale bars: 50 µm. (D-I) BrdU (D-F) and MyHC staining (G-I) after treatment with BSA (D,G) or NAb for DKK1 and DKK4 (E,H) for 3 days in *Tgfbr2*$^{fl/fl}$*;K14-Cre* palatal explants and with BSA in *Tgfbr2*$^{fl/fl}$ control palatal explants (F,I). Dotted lines indicate the outline of the TVP. Scale bars: 50 µm. (J) Quantification of the number of BrdU-labeled nuclei after treatment with BSA (blue bars) or DKK1/4 NAb (red bars) in the mesenchyme or the TVP of *Tgfbr2*$^{fl/fl}$*;K14-Cre* palatal explants and treatment with BSA in the wild-type palatal explants (green bars). Six samples per group were analyzed. ***P<0.001; NS, not significant. (K) Schematic depicts our model of the mechanism of soft palate development in wild-type (WT; upper panel) and *Tgfbr2*$^{fl/fl}$*;K14-Cre* mice (lower panel). Loss of *Tgfbr2* results in upregulated expression of *Dkk1* and *Dkk4* and inhibits WNT signaling in the palatal mesenchyme, resulting in muscle defects.

Palatal shelf organ culture

Timed-pregnant mice were sacrificed at E15.5. Genotyping was carried out as described above. The palatal shelves were micro-dissected and cultured in BGJb medium supplemented with penicillin, streptomycin, vitamin C and 10% fetal bovine serum. After 24 or 72 hours in culture with neutralizing antibodies (1 µg/ml each) for DKK1 and DKK4, or WNT inhibitor endo-IWR1 (50 µM; Tocris Bioscience), soft palate explants were fixed in 4% paraformaldehyde in 0.1 M phosphate buffer (pH 7.4) and processed for histological analysis as previously described (Iwata et al., 2012).

Whole-mount and section *in situ* hybridization

The probes for *Dkk1* and *Dkk4* were obtained from Dr Irma Thesleff (University of Helsinki, Finland). *In situ* hybridization was performed as described previously (Iwata et al., 2010). Several negative controls (e.g. sense probe and no probe) were run in parallel with the experimental reaction.

Cell culture

Primary mouse embryonic palatal mesenchymal (MEPM) cells were obtained from E13.5 embryos as described previously (Iwata et al., 2012). C2C12 cells (ATCC) were cultured in Dulbecco's modified Eagle's medium (DMEM) containing 10% fetal bovine serum supplemented with penicillin, streptomycin, L-glutamate, sodium pyruvate and nonessential amino acids. Cell proliferation assays were performed using a cell counting kit (Dojindo Molecular Technologies). MEPM and C2C12 cells were treated with endo-IWR1 (Tocris Bioscience) at 10 µM for 24 hours or left untreated. Myogenic differentiation was induced by culture in a monolayer in differentiation medium (DMEM supplemented with 2% donor equine serum, 1 µM insulin, penicillin, streptomycin and L-glutamate) for 3 or 5 days. Myofibers were stained with MyHC. All fluorescence images were obtained using a

fluorescence microscope (Model IX71, Olympus). Pictures were taken using MicroSuite Analytical Suite software (Olympus).

Statistical analysis

Two-tailed Student's *t*-tests were applied for statistical analysis. For all graphs, data are mean ± s.d. A *P*-value of less than 0.05 was considered statistically significant.

Acknowledgements

We thank Drs J. Mayo and B. Samuels for critical reading of the manuscript; Dr H. Moses for *Tgfbr2*$^{fl/fl}$ mice; Dr H. Slavkin for discussion; P. Bringas, Jr, O. Chaudhry, the Molecular Imaging Center and the Microarray core of CHLA for technical assistance.

Competing interests

The authors declare no competing financial interests.

Author contributions

J.I., A.S. and Y.C. designed research; J.I., A.S. and T.Y. performed experiments; T.-V.H., M.U. and P.A.S.-L. performed microCT imaging analysis; J.I. and Y.C. wrote the manuscript. R.P. performed the microarray analyses.

Funding

This work was supported by grants from the National Institute of Dental and Craniofacial Research [DE020065 and DE012711 to Y.C.]. Deposited in PMC for release after 12 months.

Supplementary material

Supplementary material available online at
http://dev.biologists.org/lookup/suppl/doi:10.1242/dev.103093/-/DC1

References

Back, G. W., Nadig, S., Uppal, S. and Coatesworth, A. P. (2004). Why do we have a uvula?: literature review and a new theory. *Clin. Otolaryngol. Allied Sci.* **29**, 689-693.

Brault, V., Moore, R., Kutsch, S., Ishibashi, M., Rowitch, D. H., McMahon, A. P., Sommer, L., Boussadia, O. and Kemler, R. (2001). Inactivation of the beta-catenin gene by Wnt1-Cre-mediated deletion results in dramatic brain malformation and failure of craniofacial development. *Development* **128**, 1253-1264.

Bush, J. O. and Jiang, R. (2012). Palatogenesis: morphogenetic and molecular mechanisms of secondary palate development. *Development* **139**, 231-243.

Carvajal Monroy, P. L., Grefte, S., Kuijpers-Jagtman, A. M., Wagener, F. A. and Von den Hoff, J. (2012). Strategies to improve regeneration of the soft palate muscles after cleft palate repair. *Tissue Eng. Part B Rev.* **18**, 468-477.

Chai, Y. and Maxson, R. E., Jr (2006). Recent advances in craniofacial morphogenesis. *Dev. Dyn.* **235**, 2353-2375.

Cohen, S. R., Chen, L. L., Burdi, A. R. and Trotman, C. A. (1994). Patterns of abnormal myogenesis in human cleft palates. *Cleft Palate Craniofac. J.* **31**, 345-350.

Derynck, R. and Zhang, Y. E. (2003). Smad-dependent and Smad-independent pathways in TGF-beta family signalling. *Nature* **425**, 577-584.

Dworkin, J. P., Marunick, M. T. and Krouse, J. H. (2004). Velopharyngeal dysfunction: speech characteristics, variable etiologies, evaluation techniques, and differential treatments. *Lang. Speech Hear. Serv. Sch.* **35**, 333-352.

Evans, A., Ackermann, B. and Driscoll, T. (2010). Functional anatomy of the soft palate applied to wind playing. *Med. Probl. Perform. Art.* **25**, 183-189.

Flores, R. L., Jones, B. L., Bernstein, J., Karnell, M., Canady, J. and Cutting, C. B. (2010). Tensor veli palatini preservation, transection, and transection with tensor tenopexy during cleft palate repair and its effects on eustachian tube function. *Plast. Reconstr. Surg.* **125**, 282-289.

Grenier, J., Teillet, M. A., Grifone, R., Kelly, R. G. and Duprez, D. (2009). Relationship between neural crest cells and cranial mesoderm during head muscle development. *PLoS ONE* **4**, e4381.

He, F., Xiong, W., Wang, Y., Li, L., Liu, C., Yamagami, T., Taketo, M. M., Zhou, C. and Chen, Y. (2011). Epithelial Wnt/β-catenin signaling regulates palatal shelf fusion through regulation of Tgfβ3 expression. *Dev. Biol.* **350**, 511-519.

Hilliard, S. A., Yu, L., Gu, S., Zhang, Z. and Chen, Y. P. (2005). Regional regulation of palatal growth and patterning along the anterior-posterior axis in mice. *J. Anat.* **207**, 655-667.

Iwata, J., Hosokawa, R., Sanchez-Lara, P. A., Urata, M., Slavkin, H. and Chai, Y. (2010). Transforming growth factor-beta regulates basal transcriptional regulatory machinery to control cell proliferation and differentiation in cranial neural crest-derived osteoprogenitor cells. *J. Biol. Chem.* **285**, 4975-4982.

Iwata, J., Parada, C. and Chai, Y. (2011). The mechanism of TGF-β signaling during palate development. *Oral Dis.* **17**, 733-744.

Iwata, J., Hacia, J. G., Suzuki, A., Sanchez-Lara, P. A., Urata, M. and Chai, Y. (2012). Modulation of noncanonical TGF-β signaling prevents cleft palate in Tgfbr2 mutant mice. *J. Clin. Invest.* **122**, 873-885.

Iwata, J., Suzuki, A., Pelikan, R. C., Ho, T. V., Sanchez-Lara, P. A., Urata, M., Dixon, M. J. and Chai, Y. (2013a). Smad4-Irf6 genetic interaction and TGFβ-mediated IRF6 signaling cascade are crucial for palatal fusion in mice. *Development* **140**, 1220-1230.

Iwata, J., Suzuki, A., Pelikan, R. C., Ho, T. V. and Chai, Y. (2013b). Noncanonical transforming growth factor β (TGFβ) signaling in cranial neural crest cells causes tongue muscle developmental defects. *J. Biol. Chem.* **288**, 29760-29770.

Jin, Y. R., Han, X. H., Taketo, M. M. and Yoon, J. K. (2012). Wnt9b-dependent FGF signaling is crucial for outgrowth of the nasal and maxillary processes during upper jaw and lip development. *Development* **139**, 1821-1830.

Karaman, M. W., Houck, M. L., Chemnick, L. G., Nagpal, S., Chawannakul, D., Sudano, D., Pike, B. L., Ho, V. V., Ryder, O. A. and Hacia, J. G. (2003). Comparative analysis of gene-expression patterns in human and African great ape cultured fibroblasts. *Genome Res.* **13**, 1619-1630.

Kawano, Y. and Kypta, R. (2003). Secreted antagonists of the Wnt signalling pathway. *J. Cell Sci.* **116**, 2627-2634.

Lan, Y. and Jiang, R. (2009). Sonic hedgehog signaling regulates reciprocal epithelial-mesenchymal interactions controlling palatal outgrowth. *Development* **136**, 1387-1396.

Marsh, J. L. (1991). Cleft palate and velopharyngeal dysfunction. *Clin. Commun. Disord.* **1**, 29-34.

Massagué, J. and Chen, Y. G. (2000). Controlling TGF-beta signaling. *Genes Dev.* **14**, 627-644.

Mukhopadhyay, M., Shtrom, S., Rodriguez-Esteban, C., Chen, L., Tsukui, T., Gomer, L., Dorward, D. W., Glinka, A., Grinberg, A., Huang, S. P. et al. (2001). Dickkopf1 is required for embryonic head induction and limb morphogenesis in the mouse. *Dev. Cell* **1**, 423-434.

Nie, X., Luukko, K., Fjeld, K., Kvinnsland, I. H. and Kettunen, P. (2005). Developmental expression of Dkk1-3 and Mmp9 and apoptosis in cranial base of mice. *J. Mol. Histol.* **36**, 419-426.

Perry, J. L. (2011). Anatomy and physiology of the velopharyngeal mechanism. *Semin. Speech Lang.* **32**, 83-92.

Pounds, S. and Cheng, C. (2004). Improving false discovery rate estimation. *Bioinformatics* **20**, 1737-1745.

Precious, D. S. and Delaire, J. (1993). Clinical observations of cleft lip and palate. *Oral Surg. Oral Med. Oral Pathol.* **75**, 141-151.

Semënov, M. V., Tamai, K., Brott, B. K., Kühl, M., Sokol, S. and He, X. (2001). Head inducer Dickkopf-1 is a ligand for Wnt coreceptor LRP6. *Curr. Biol.* **11**, 951-961.

Smyth, G. K. (2004). Linear models and empirical bayes methods for assessing differential expression in microarray experiments. *Stat. Appl. Genet. Mol. Biol.* **3**, Article3.

Snider, L. and Tapscott, S. J. (2003). Emerging parallels in the generation and regeneration of skeletal muscle. *Cell* **113**, 811-812.

Thomason, H. A., Zhou, H., Kouwenhoven, E. N., Dotto, G. P., Restivo, G., Nguyen, B. C., Little, H., Dixon, M. J., van Bokhoven, H. and Dixon, J. (2010). Cooperation between the transcription factors p63 and IRF6 is essential to prevent cleft palate in mice. *J. Clin. Invest.* **120**, 1561-1569.

van der Sloot, P. G. (2003). Hard and soft palate reconstruction. *Curr. Opin. Otolaryngol. Head Neck Surg.* **11**, 225-229.

Wang, Y., McClelland, M. and Xia, X. Q. (2009). Analyzing microarray data using WebArray. *Cold Spring Harb. Protoc.* **2009**, pdb prot5260.

Xia, X., McClelland, M. and Wang, Y. (2005). WebArray: an online platform for microarray data analysis. *BMC Bioinformatics* **6**, 306.

Xu, X., Han, J., Ito, Y., Bringas, P., Jr, Urata, M. M. and Chai, Y. (2006). Cell autonomous requirement for Tgfbr2 in the disappearance of medial edge epithelium during palatal fusion. *Dev. Biol.* **297**, 238-248.

Xu, X., Han, J., Ito, Y., Bringas, P., Jr, Deng, C. and Chai, Y. (2008). Ectodermal Smad4 and p38 MAPK are functionally redundant in mediating TGF-beta/BMP signaling during tooth and palate development. *Dev. Cell* **15**, 322-329.